The Journal of Immunology

RESEARCH ARTICLE | AUGUST 01 2001

Kinetic Analysis of the Interactions of Complement Receptor 2 (CR2, CD21) with Its Ligands C3d, iC3b, and the EBV Glycoprotein gp350/220[1]

Maria Rosa Sarrias; ... et. al

J Immunol (2001) 167 (3): 1490–1499.
https://doi.org/10.4049/jimmunol.167.3.1490

Kinetic Analysis of the Interactions of Complement Receptor 2 (CR2, CD21) with Its Ligands C3d, iC3b, and the EBV Glycoprotein gp350/220[1]

Maria Rosa Sarrias,[2]* Silvia Franchini,* Gabriela Canziani,† Emelia Argyropoulos,* William T. Moore,* Arvind Sahu,‡ and John D. Lambris[3]*

The molecular mechanisms involved in the interaction of complement receptor 2 (CR2) with its natural ligands iC3b and C3d are still not well understood. In addition, studies regarding the binding site(s) of the receptor on C3 as well as the affinities of the C3 fragments for CR2 have produced contradictory results. In the present study, we have used surface plasmon resonance technology to study the interaction of CR2 with its ligands C3d, iC3b, and the EBV surface glycoprotein gp350/220. We measured the kinetics of binding of the receptor to its ligands, examined the influence of ionic contacts on these interactions, and assessed whether immobilized and soluble iC3b bound with similar kinetics to CR2. Our results indicate that 1) gp350 binding to CR2 follows a simple 1:1 interaction, whereas that of the C3 fragments is more complex and involves more than one intramolecular component; 2) kinetic differences exist between the binding of C3d and iC3b to CR2, which may be due to an additional binding site found on the C3c region of iC3b; and 3) iC3b binds to CR2 with different kinetics, depending on whether the iC3b is in solution or immobilized on the surface. These findings suggest that binding of CR2 to iC3b and C3d is more complex than previously thought. *The Journal of Immunology,* **2001, 167: 1490–1499.**

Complement receptor 2 (CR2,[4] CD21) is a 145-kDa type I transmembrane glycoprotein that is expressed primarily on mature B lymphocytes, epithelial cells, thymocytes, and follicular dendritic cells (1–5). This receptor belongs to the regulators of complement activation family of proteins. It is composed of an ectodomain, which is comprised of 15 or 16 short consensus repeat (SCR) or complement control protein (CCP) domains depending on the splice site usage, a 24 aa transmembrane region, and a 34-residue cytoplasmic tail (6, 7).

A role for CR2 has been invoked in B cell activation, the generation of immunologic memory, Ig class switching, and B cell tolerance (1–4, 6–11). Binding of CR2 to its natural ligands (C3d or iC3b) attached to an Ag, immune complex, or pathogen as a consequence of complement activation, triggers the immunological responses of the receptor (8, 12). Coupling of an Ag to two or three copies of C3d has been shown to elicit a 1,000- or 10,000-fold enhanced T-dependent B cell response (13, 14). It is believed that this enhancement of the humoral response is the result of enhanced retention of Ag by follicular dendritic cells in germinal centers and of enhanced recruitment of the CR2/CD19/CD81 coreceptor into the B cell-Ag receptor complex (8, 12). In addition to iC3b and C3d, the EBV surface glycoprotein gp350/220 also binds to CR2, and mediates EBV infection of CR2-expressing cells (15–17). It is noteworthy that several cellular responses with similar characteristics of the C3d-CR2 interaction have been observed upon gp350/220 binding to CR2 (18–20). Specifically, gp350/220 has been shown to induce B cell proliferation (19), and when coupled to an Ag (monoclonal anti-human IgD Ab), it was found to enhance membrane Ig-mediated B cell stimulation in vitro (20). The similarities between the binding of gp350 and the C3 fragments to CR2 extend even further. The binding site for iC3b, C3d, and gp350 has been located in the N-terminal SCR 1 and 2 domains of the receptor (21, 22). Furthermore, the viral protein competes with C3d and iC3b for interaction with CR2.

Based on mAb competitions, peptide mapping, and site-directed mutagenesis studies, it has been determined that the CR2 binding site on gp350/220 lies within residues 1–470 of the viral glycoprotein. Specifically, a mAb that binds to this region (72 A1) inhibits gp350/220 binding to CR2 and viral entry into host cells (15, 23). Furthermore, a peptide that binds to CR2 has been identified within this fragment of the molecule (aa 21–30, EDPGFFNVEI) (15), and deletion of aa 28 and 29 in this region (VE) abolishes the binding of gp350/220 to CR2 (23).

Whether CR2 binds to C3 at a single or multiple sites is controversial. Chemical fragmentation and peptide mapping have identified a region on C3d, aa 1199–1210 (mature C3 numbering) to which CR2 binds (24). A polymeric synthetic peptide K^{1187}-A^{1214} (KFLTTAKDKNRWEDPFKQLYNVEATSKYA) binds to CR2 on Raji cells (24) and stimulates cell proliferation (18, 25, 26). Furthermore, when a peptide (equivalent to residues 1195–1210 of C3) was

*Protein Chemistry Laboratory, Department of Pathology and Laboratory Medicine, and †Department of Medicine, School of Medicine, University of Pennsylvania, Philadelphia, PA 19104; and ‡National Centre for Cell Science, Pune University Campus, Ganeshkhind, Pune, India

Received for publication February 2, 2001. Accepted for publication May 25, 2001.

The costs of publication of this article were defrayed in part by the payment of page charges. This article must therefore be hereby marked *advertisement* in accordance with 18 U.S.C. Section 1734 solely to indicate this fact.

[1] This work was supported by National Institutes of Health Grant AI 30040, and Cancer and Diabetes Centers Core Support Grants CA 16520 and DK 19525. A.S. is a Wellcome Trust Overseas Senior Research Fellow in Biomedical Science in India.

[2] This work was in partial fulfillment of a PhD thesis (M.R.S.), which will be submitted to the Department of Cell Biology, Physiology, and Immunology, Universitat Autònoma de Barcelona, Spain.

[3] Address correspondence and reprint requests to Dr. John D. Lambris, Protein Chemistry Laboratory, Department of Pathology and Laboratory Medicine, 401 Stellar-Chance Laboratories, University of Pennsylvania, Philadelphia, PA 19104. E-mail address: lambris@mail.med.upenn.edu

[4] Abbreviations used in this paper: CR, complement receptor; SCR, short consensus repeat; BCCP, biotin carboxyl carrier protein; Ni-NTA, nickel-nitro acetic acid; TFA, trifluoroacetic acid; PEO, polyethylene oxide; RU, resonance units; SPR, surface plasmon resonance; Fc1, flow cell one; Fc2, flow cell two; BirA, biotin holoenzyme synthetase.

0022-1767/01/$02.00

coupled to anti-idiotype Ab, it induced a strong idiotype and Ag-specific response in mice (27). This peptide is homologous in sequence to the CR2-binding region on gp350/220. The observation that synthetic peptides representing aa 295–306 (β-chain) and 744–755 (α-chain) showed similarity to the above peptide of C3 that binds to CR2 (25) suggested that additional residues in C3 might participate in the interaction with CR2. These peptides were identified based on their sequence homology with the C3d residues 1201–1214, and the binding was corroborated by the ability of peptides and C3c immobilized to microspheres to bind to Raji cells through CR2 (25).

Kalli and coworkers (28) have shown that soluble C3d and iC3b inhibit soluble CR2 binding to iC3b-coated erythrocytes to a similar extent. The authors thus concluded that the interaction between CR2 and C3 is delimited to the C3d region. In view of this conclusion and in an effort to map the CR2 binding sites on C3, mutagenic scan studies have been performed in which erythrocytes coated with mutated iC3b were tested for their ability to bind to soluble CR2 and induce the rosetting of CR2-bearing Raji cells. In these studies, mutagenesis of residues 1199–1210 (EDPFKQLYNVEA) was shown to reduce the binding of iC3b to CR2 by only 20% (29). The recent availability of the x-ray crystallographic structure of C3d has indicated the presence of a negatively charged pocket on the concave surface of the molecule (30). The authors of this x-ray crystallographic study proposed this pocket as a candidate site for CR2 interaction. Replacement of two clusters of negatively charged C3d residues (E37^{1008}/E39^{1010}, and E160^{1131}/D163^{1134}/E166 ^{1137}, C3d numbering, mature C3 numbering) present on the opposite side of the acidic pocket led to severe inhibition of the interaction (31).

Because the results of the localization of the C3 binding sites for CR2 are apparently contradictory, it is not clear whether the interaction between CR2 and C3 is mediated only through the C3d region or other regions in C3 are involved in the interaction. In addition, it is not clear whether C3d interacts with CR2 through single or multiple sites and whether differences in experimental settings may affect these interactions. In the present study, we have analyzed the kinetics of the interaction of CR2 with C3d and iC3b in real time using surface plasmon resonance (SPR) and have asked whether these interactions are similar in nature. Because gp350 also serves as a ligand for CR2, we have analyzed its interaction with CR2 and have compared this interaction with those of CR2 with C3d and iC3b. Our results indicate that the binding of CR2 to viral gp350 follows a simple 1:1 binding model, whereas its binding to the C3 fragments is more complex. We observed direct binding of CR2 to a synthetic peptide with a sequence comprising C3 amino acids K^{1187}-A^{1214}, suggesting that this region in C3d is involved in its interaction with the receptor. We have also detected kinetic differences between the binding of iC3b and C3d to CR2. Finally, we observed direct binding of CR2 to the C3c fragment, which suggests that the regions of iC3b and C3d involved in their interaction with CR2, in addition to common contact sites, may involve regions that differ from each other.

Materials and Methods

Recombinant proteins

In this study we have expressed a truncated form of EBV gp350/220 (gp350 (470t)), the ectodomain of CR2 (soluble CR2 containing SCR 1–15), and soluble CR2 in fusion with biotinylation tag (CR2-BCCP) using the baculovirus system. The cloning procedure for the expression of soluble CR2 in the baculovirus system has been described elsewhere (32). This clone was a gift from Michael Holers (Department of Medicine and Immunology, University of Colorado Health Science Center, Denver, CO). The EBV gp350 (470t) and CR2-BCCP expression constructs were cloned as follows: to obtain gp350, the gp350 (470t) cDNA was amplified by the PCR from the pGEM-gp350 clone (33) using the primers 5′-TCGG GA TCCA ATG GAG GCA GCC TTG ATT GTG TGT CAG TA-3′ (forward) and 5′-CCT GCGGCCGC CTA ATG GTG ATG GTG ATG GTG GGA T GAT ACA GTG GGG CCT GT-3′ (reverse), which added six C-terminal His codons and a stop codon. The His codons were added to provide a binding site for the nickel-nitro acetic acid (Ni-NTA)-agarose resin (Qiagen, Chatsworth, CA) used in the purification of the expressed protein. The PCR-amplified product was cloned into the pVT-Bac vector (34), which contains the honeybee mellitin signal sequence. CR2-BCCP is composed of a CR2 molecule (SCR 1–15) fused at its C terminus to residues 70–156 of the biotin carboxyl carrier protein (BCCP) from *Escherichia coli* (35). The construction of this clone involved several steps. First, total DNA was extracted from an overnight culture of *E. coli* DH5α cells. The cDNA encoding the BCCP protein was then amplified by PCR using the primers 5′-AAC TGA GCT CAT GGA AGC GCC AGC AGC A-3′ (forward) and 5′-ATT AGC TAG CCT ACT CGA TGA CGA CCA GCG G-3′ (reverse) and cloned into the pVT-Bac vector (pVT-Bac-BCCP). The CR2 cDNA was then PCR-amplified from the pGEM-CR2 clone (32) with primers 5′-AAT TCC CGG GAT GGG CGC CGC GGG CCT G-3′ and 5′-CAC GAG CTC TGA ACG GGA TCT GCA AAC-3′ and cloned into the pVT-Bac-BCCP construct, in-frame with the BCCP protein.

The resulting gp350 (470t) and CR2-BCCP constructs were recombined into baculovirus (*Autographa californica* nuclear polyhedrosis virus) by cotransfection with Baculogold DNA (PharMingen, San Diego, CA). Recombinant plaques were isolated and amplified, and the resulting culture supernatants were screened for protein expression by SDS-PAGE and Western blotting. Baculovirus recombinants expressing the protein of interest were subjected to two additional rounds of plaque purification. For production of larger quantities of protein, *Spodoptera frugiperda* Sf9 cells (Life Technologies, Gaithersburg, MD) grown in suspension cultures were infected at a multiplicity of infection of 4. Forty-eight to 72 h after infection the supernatants were cleared by centrifugation, concentrated, and then dialyzed against PBS.

The baculovirus-expressed recombinant proteins were purified by using Ni-NTA agarose or mAb HB5 affinity columns. The His-tagged protein gp350 (470t) was affinity-purified over an Ni-NTA-agar column. The bound protein was eluted with increasing concentrations of imidazole (0.01–0.25 M) in 0.02 M phosphate buffer (pH 7.5) with 0.5 M NaCl. The other two recombinant proteins (CR2 and CR2-BCCP) were affinity-purified over a Sepharose column covalently coupled to mAb HB5 specific for CR2 (American Type Culture Collection, Manassas, VA). Soluble CR2 was further purified over a protein G-Sepharose column to remove traces of HB5 Ab that might have leaked from the column. The eluates from all purifications were dialyzed against PBS and concentrated using the Amicon (Beverly, MA) ultrafiltration system.

The biotin holoenzyme synthetase protein, BirA, catalyzes the incorporation of biotin into BCCP. This protein was expressed in *E. coli* using a clone that was provided by Dr. D. Beckett (Department of Chemistry and Biochemistry, University of Maryland, College Park, MD) (36). The expressed protein was affinity-purified over an Ni-NTA-agar column by eluting with increasing concentrations of imidazole (0.01–0.25 M) in 0.02 M phosphate buffer (pH 7.5) with 0.5 M NaCl. The eluted protein was dialyzed overnight into a buffer solution containing 200 mM KCl with 50 mM Tris and 5% glycerol (pH 7.5).

Serum proteins

C3 (37) and factors I (38) and H (39) were purified from human serum as previously described. To obtain C3b or C3c and C3d, C3 was cleaved at 37°C with 1% w/w trypsin for 10 min, or 5% w/w trypsin for 1 h, respectively (40). The reactions were stopped by adding a 3-fold (w/w) excess of soybean trypsin inhibitor over the amount of trypsin used. To obtain iC3b, 500 μg of C3b was incubated with 150 μg of factor H and 64 μg of factor I for 4 h at 37°C. C3b, C3d, C3c, and iC3b were purified on a Mono Q column and gel filtration (Pharmacia, Piscataway, NJ) as previously described (41, 42).

Peptide synthesis, purification, and characterization

The peptide with the C3 sequence K^{1187}-A^{1214} (Biotin-K F L T T A K D L N R W E D P G K Q L Y N V E A T S Y A) corresponding to C3 residues 1187–1214 (24) and a control peptide (Biotin-G S G S K P F P A P Q T P G R L Q P A P V I P S A P A A P) were synthesized in an Applied Biosystems (Foster City, CA) peptide synthesizer (model 431A) using F-moc amide resin (4-(2′,4′-dimethoxyphenyl-F-moc-aminomethyl)-phenoxy resin). The side chain-protecting groups were Asp (otBu), Arg (Pmc), Thr (tBu), Gln (Trt), and Trp (Boc). Biotin (1 mmol) was dissolved in equal

volumes of DMSO and *N*-methylpyrrolidone, placed in an amino acid cartridge, and activated according to Applied Biosystems User Bulletin no. 35 before carrying on the peptide synthesis. The peptides were cleaved from the resin by incubation for 3 h at 22°C with a solvent mixture containing 5% phenol, 5% thioanisole, 5% water, 2.5% ethanedithiol, and 82.5% trifluoroacetic acid (TFA). The reaction mixture was filtered through a fritted funnel, precipitated with cold ether, dissolved in 50% acetonitrile containing 0.1% TFA, and lyophilized. The crude peptides obtained after cleavage were dissolved in 10% acetonitrile containing 0.1% TFA and purified using a reversed-phase C-18 column (Waters, Milford, MA). The purity of all peptides was monitored by analytical chromatography on a reversed-phase C-18 column and by laser desorption mass spectrometry (43).

Protein sequencing and mass spectrometry

To obtain the NH_2-terminal sequence of gp350 (470t), the protein was subjected to electrophoresis and electroblotted onto a Problot membrane (PerkinElmer-Applied Biosystems, Foster City, CA). After the bands were excised from the membrane, automated Edman degradation was performed with the PerkinElmer-Applied Biosystems model 473A Protein Sequencer equipped with on-line phenylthiohydantoin-amino acid analysis, using programmed chemistry cycles and HPLC operation programs provided by the manufacturer. For mass spectrometric analysis, gp350 (470t) and soluble CR2 were desalted using a matrix para-crystalline method previously described (43), and thereafter subjected to matrix-assisted laser desorption ionization-mass spectrometry analysis using a Micromass (Beverly, MA) TofSpec 2E time-of-flight mass spectrometer (1.0 m flight tube) equipped with a nitrogen laser (337 nm).

Site-specific biotinylation of CR2-BCCP and C3

To incorporate biotin at a single residue on CR2-BCCP and C3, the following strategies were used: 1) CR2-BCCP labeling was achieved in the presence of the BirA protein, which catalyzed the reaction; and 2) the labeling of C3 and its fragments was performed using the sulfhydryl-reactive EZ-Link polyethylene oxide (PEO)-maleimide-activated biotin (Pierce, Rockford, IL).

For labeling, CR2-BCCP was first dialyzed using 40 mM Tris-Cl, 5.5 mM $MgCl_2$, and 100 mM KCl (pH 8) and then 31 μM of the protein was incubated with 365 μM of the BirA protein, 24 μg of d-biotin (Sigma, St. Louis, MO), and 20 mM ATP (Sigma) for 1 h at 37°C. Excess unincorporated biotin was removed from the reaction mixture by PD-10 column (Amersham Pharmacia Biotech, Uppsala, Sweden) gel filtration chromatography and extensive dialysis against PBS. The specificity of this reaction was determined by using soluble CR2 as a control.

Human C3 and C3 fragments were biotinylated as follows. The thioester bond of native C3 was hydrolyzed by incubating 7.8 mg of C3 (43 μM) with an equal volume of a 0.2 M solution of methylamine (pH 7.3) overnight at 37°C (44–46). The buffer was then exchanged into a solution consisting of 0.1 M NaH_2PO_4 and 5 mM EDTA (pH 6.3) by using a PD-10 column (Amersham Pharmacia Biotech). EZ-Link PEO-maleimide-activated biotin (Pierce) was dissolved in PBS at a concentration of 10 mM and then added to the C3 protein suspension at a 5:1 molar ratio. The reaction mixture was incubated for 30 min at room temperature, and then the sample was desalted and exchanged into PBS twice over a PD-10 column to remove the free biotin. The C3 fragments C3b, iC3b, and C3d were obtained by limited tryptic cleavage of the same stock of biotinylated C3 protein as described above. Monitoring of the biotinylation reactions, cleavages, and purifications was performed with SDS-PAGE and Western blotting.

Western blot assays

Proteins were separated on SDS-PAGE and electrotransferred to a nitrocellulose membrane. Nonspecific binding to the membrane was prevented by incubation in blocking buffer (PBS containing 10% milk). For CR2 detection, the membranes were incubated with a monoclonal anti-CR2 Ab (HB5, 2 μg/ml); gp350 (470t) was detected with a 1/5000 dilution of an anti-His tag (C-terminal) mAb (Invitrogen, Carlsbad, CA) or a 1/500 dilution of a polyclonal anti-EBV Ab (provided by Dr. Michael Holers). Bound mAbs were detected with a peroxidase-labeled goat-anti mouse IgG Ab (Bio-Rad, Richmond, CA), and bound polyclonal Abs were detected with a peroxidase-labeled mouse anti-rabbit Ab (Bio-Rad). The incorporation of biotin was verified by reactivity with peroxidase-labeled streptavidin (Life Technologies). All of these incubation steps were performed for 1 h at 22°C, and the membranes were washed with PBS containing Tween 20 (0.05%) between each incubation step. The proteins were detected using the ECL kit (Amersham Pharmacia Biotech).

SPR measurements

The kinetics of CR2 binding to its ligands C3d, iC3b, gp350, $C3^{1187–1214}$ peptide, and C3c were determined on the SPR-based biosensor BIAcore X (BIAcore, Piscataway, NJ). All the experiments were performed at 25°C in phosphate buffer containing 0.05% Tween 20 (pH 7.4), either at physiologic ionic strength (150 mM NaCl), or in 75 mM NaCl. To orient C3d, iC3b, CR2, and $C3^{1187–1214}$ peptide onto the chip and thus obtain a homogeneous ligand surface, the proteins were biotinylated at a specific residue as previously described and then immobilized on a streptavidin chip (Sensor Chip SA; BIAcore). C3c was immobilized on a CM5 chip by using amine-coupling chemistry (Sensor Chip SA). One hundred forty resonance units (RU) of CR2, 250 RU of C3d, 350 RU of iC3b, 2800 RU of C3c, or 500 RU of $C3^{1187–1214}$ peptide were immobilized on flow cell two (Fc2). Flow cell one (Fc1) was used as a blank control, except for the binding experiments involving the $C3^{1187–1214}$ peptide, in which a biotinylated control peptide was immobilized on Fc1. Binding was measured at 50 μl/min to avoid mass transport effects. At this flow the initial on-rate was maximum. Flow was allowed to occur for several seconds to establish a baseline, and then various concentrations of analyte were injected and the association was followed for 120 s. At that time, sample was replaced with running buffer, and the dissociation of the complex was monitored for 240 s. The sensor chip was regenerated with brief pulses of 0.2 M sodium carbonate (pH 9.5). The activity of the immobilized protein was monitored by observing the binding response of a single concentration of analyte throughout the experiment. Biosensor data for the control Fc1 were subtracted from those obtained for the immobilized proteins. Each binding experiment was performed at least twice, and the responses were averaged. Several buffer injections were also performed, averaged, and subtracted from Fc2 signal. BIAevaluation 3.0 (BIAcore) software was used to analyze the binding data, using global fitting. Linear analysis of the binding data was obtained as previously described (46–48) by plotting d*R*U/d*t* vs RU, where RU is the relative response of the biosensor at time *t*. The apparent equilibrium dissociation constant (K_D) was calculated from the equation $K_D = k_{off}/k_{on}$.

Results

Characterization of the recombinant proteins

To analyze the interaction of CR2 with its ligands, we expressed both the receptor and its ligand gp350 (470t) using the baculovirus system. Because previous studies had shown that EBV gp350/220, when truncated at residue 470, can inhibit EBV binding to CR2 (23), we chose to express this gp350 (470t) construct for use in the interaction analysis. A C-terminal His tag was added to this protein to aid in its purification. gp350 (470t) does not have a well-defined signal peptide. To verify whether its putative signal peptide had been processed, we sequenced its N terminus. Edman degradation yielded the sequence DPMEAALIV, with DP being the amino acids added in the cloning process and MEAALIV the putative signal peptide. Thus, its putative signal peptide had not undergone cleavage upon secretion of the protein. The molecular size of gp350 (470t) as predicted from the amino acid sequence of the protein was 50 kDa. However, analysis by SDS-PAGE and Western blot revealed a band of 65–70 kDa (Fig. 1). Mass spectrometric analysis showed a single homogeneous species and indicated that the gp350 (470t) had a total mass of 72 kDa (Fig. 1*A*). Because this protein contains 18 potential N-glycosylation sites, we conclude that glycosylation contributed 20 kDa to the total size of the molecule. This conclusion is consistent with previous studies of the gp350 protein, which have indicated that it is heavily glycosylated (23, 49, 50).

Expression of soluble recombinant CR2 in the baculovirus system has been previously reported (32). Purified soluble CR2 was analyzed by SDS-PAGE, Western blotting, and mass spectrometry. The recombinant soluble CR2 had a molecular size of 116 kDa, (Fig. 1*B*) which does not differ substantially from the size deduced from its amino acid composition (111 kDa). It is possible that associated carbohydrates added 5 kDa of mass because CR2 contains eleven putative sites of N-glycosylation. The recombinant CR2-BCCP was analyzed by SDS-PAGE and Western blotting.

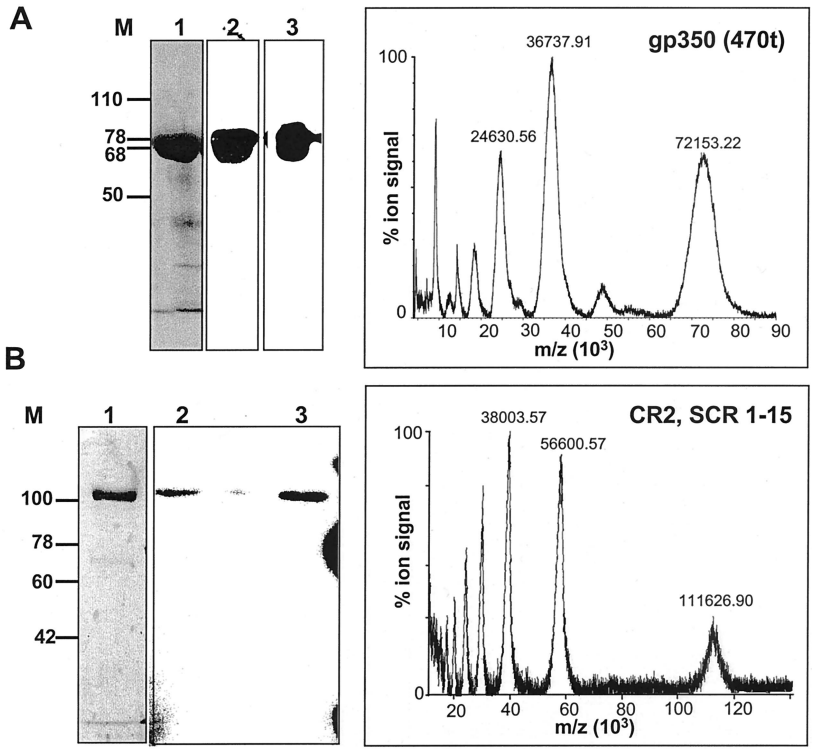

FIGURE 1. SDS-PAGE, Western blotting, and mass spectrometry of gp350 (470t), CR2, and CR2-BCCP. The purified proteins were subjected to SDS-PAGE and stained with Coomassie blue or transferred to a nitrocellulose membrane and probed with specific Abs. gp350 (470t) and CR2 were also analyzed by mass spectrometry. *A, left, lane 1*, Coomassie blue-stained gp350 (470t); *lanes 2* and *3*, reactivity of gp350 (470t) with a mAb anti-His tag or a polyclonal Ab anti-EBV, respectively. *A, right*, Mass spectrometric analysis of purified gp350 (470t). *B, left, lane 1*, Coomassie blue-stained, purified soluble CR2; *lanes 2* and *3*, reactivity of purified CR2-BCCP and soluble CR2, respectively, with the monoclonal anti-CR2 Ab HB5. The molecular mass marker (kDa) is indicated in *lane M*. *B, right*, Mass spectrometric analysis of purified CR2, SCR 1–15.

Purified CR2-BCCP migrated as a single band, as visualized by its reactivity with mAb HB5 (Fig. 1).

Generation and characterization of site-specific biotinylated proteins

To measure the affinity and binding kinetics of the interaction between CR2 and its ligands, we used SPR technology. In such studies, immobilization of the ligand is generally achieved by the use of amine-coupling chemistry. However, this approach produces heterogeneous surface ligands and precludes the measurement of homogeneous binding kinetics. To overcome this problem, we designed an enzymatic and a chemical strategy to incorporate biotin at a specific residue on CR2 and C3, respectively (Fig. 2). This strategy provided a means of orienting these proteins on a

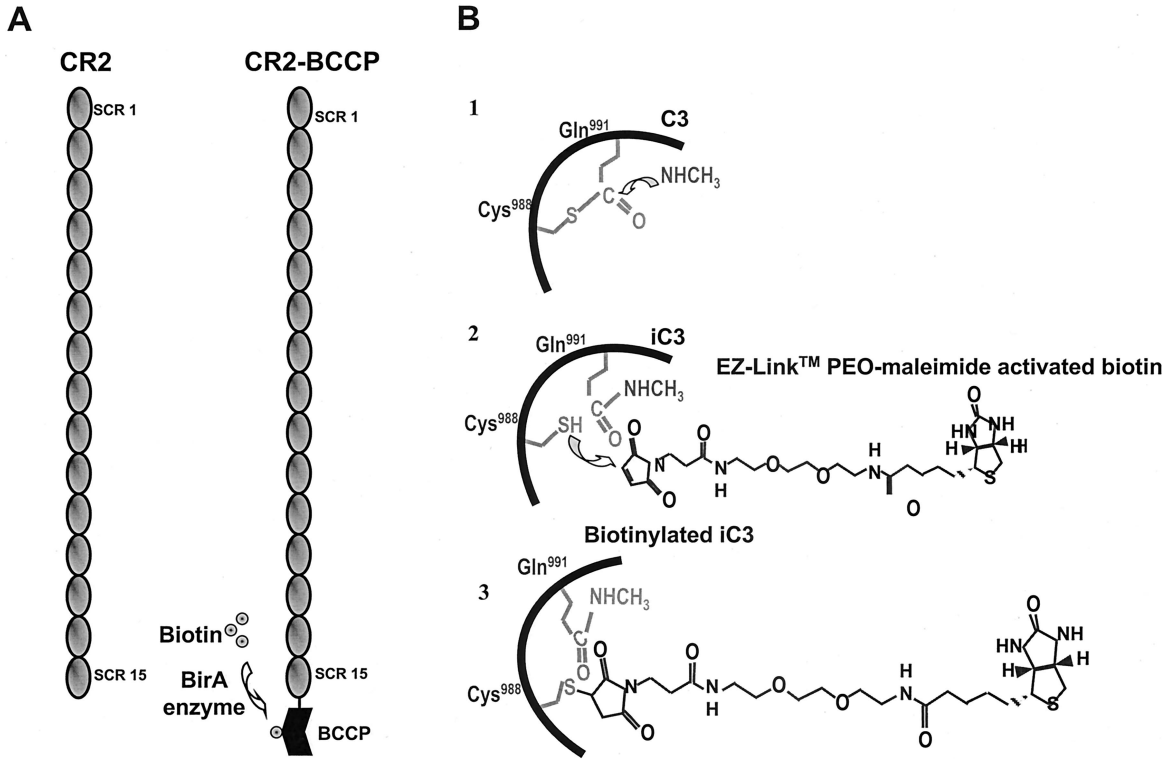

FIGURE 2. Diagram depicting the strategies used for site-specific biotinylation of CR2 and the C3 fragments. CR2 was expressed in fusion of a biotinylation tag in its C terminus (*A*), whereas C3 was biotinylated in its thioester site and subsequently cleaved to its fragments iC3b and C3d (*B*).

streptavidin sensor chip surface in a way mimicking their physiological orientation.

To allow for site-specific biotinylation on the CR2 molecule, we cloned and expressed a CR2 protein in fusion with aa 70–156 of the BCCP from *E. coli* (35) at its C terminus. BCCP is a subunit of the *E. coli* enzyme acetyl-CoA carboxylase and contains a single, specific K residue that acts as a biotin acceptor (35, 36, 51). Therefore, this construct allowed us to incorporate biotin at a single residue on the C-terminal tag of CR2. The CR2-BCCP was labeled with biotin on its C-terminal BCCP tag, in the presence of the catalyzing enzyme BirA and ATP. To verify that the reaction was specific, we used recombinant CR2 as a negative control. We then analyzed biotin incorporation into both molecules by Western blotting. As shown in Fig. 3, only CR2-BCCP reacted with peroxidase-labeled streptavidin, indicating that only the BCCP-tagged protein had incorporated biotin.

To orient the C3 fragments C3d and iC3b on a BIAcore chip, they were biotinylated at Cys^{988}, which participates in the formation of the thioester bond. Biotin was incorporated into the thiol group after hydrolysis of the thioester bond with methylamine. Following biotin incorporation, the biotinylated C3 was cleaved into its degradation fragments iC3b and C3d. The iC3b and C3d were generated from the same stock of biotinylated C3 to ensure that any differences in our BIAcore data that we obtained for the two molecules were not related to heterogeneity at the biotinylation stage. To verify that only the -SH group of Cys^{988} had incorporated biotin, we analyzed the reactivity of C3d and iC3b with peroxidase-labeled streptavidin in a Western blot (Fig. 3). Biotin incorporation was detected mainly in the fragments containing Cys^{988} (i.e., the 68-kDa fragment of iC3b and C3d).

Kinetic analysis of the interaction of CR2 with iC3b, C3d, and gp350

In the present study, we have examined the interaction of CR2 with its ligands by SPR technology using a BIAcore X biosensor, and we addressed the following: 1) whether C3d and iC3b have different affinities for soluble and surface-bound CR2; and 2) whether the affinities of CR2 for fluid-phase and surface-attached C3d/iC3b (e.g., when C3d/iC3b are attached to complement-activating particles) can vary as a result of differential exposure of interacting residues. Thus we tested these possibilities by measuring the binding of iC3b and gp350 to CR2 immobilized on the sensor chip as well as the interaction of soluble CR2 with iC3b and C3d immobilized on the sensor chip.

When we examined the binding of gp350 (470t) to CR2 immobilized on the sensor chip, we found that the binding reaction was dose-dependent and saturable. Analysis of the binding data by global fitting analysis (BIAevaluation software 3.0) showed a close fit to 1:1 Langmuir binding model ($A + B \leftrightarrow AB$; Fig. 4*A*). A random distribution of residuals and a χ^2 value for this interaction of 1.8 indicated that this model describes well the experimental data.

Next, we evaluated the interaction of CR2 with its natural ligands, the C3 fragments C3d and iC3b. Experiments were performed in which soluble C3d and iC3b were allowed to bind to CR2 immobilized on the sensor chip. Only the kinetics of iC3b binding was further analyzed. The data corresponding to soluble C3d binding to immobilized CR2 were not reproducible and were not included in the present study. We also examined the converse arrangement, in which soluble CR2 was injected onto a chip containing bound C3d or iC3b. When we analyzed these binding reactions using the 1:1 model the global fit of the data was not possible. Although the residual plot for the fitted data and the χ^2 values were <2, the values obtained for the maximum response (R_{max}) were lower than the predicted values, and even lower than the observed response values. Eliminating the refractive index (*Ri*) parameter that ascribes a bulk to the interaction resulted in a χ^2 value >120. Linear transformation of the binding data showed nonlinear plots (Fig. 4, *B–D*), indicating that the binding follows complex models.

Data from our laboratory and others have indicated that two regions of CR2 (52, 53) and more than one region of C3d/iC3b (24, 25, 29, 31, 54) may be involved in C3d/iC3b-CR2 interactions. Thus, it is possible that two regions of C3d/iC3b may interact with two regions of CR2. To test this possibility, we tried to fit our data to a bivalent analyte model: $AA + B \leftrightarrow AAB$; $AAB + B \leftrightarrow AABB$ (Fig. 4). These data include binding of CR2 to immobilized iC3b and C3d and binding of iC3b to immobilized CR2. The latter experiment was performed in the presence of 75 mM NaCl in the binding buffer, which allowed us to observe better binding. For these analyses, the residual plot for the fitted data and the χ^2 values ranged from 1 to 3 and from 1.5 to 2.1, respectively, and the residuals were randomly distributed around the fit. Besides, the R_{max} values were close to the predicted maximum response. Other models, such as a conformational change model, did not describe the data obtained. A two-step binding model describes well the binding data where two or more binding steps are affecting the binding equilibrium between CR2 and C3d or between CR2 and iC3b. The overlaid data, with the result of the global fitting analysis for a bivalent model for iC3b binding to immobilized CR2, are shown in Fig. 4*B*, and those for the binding of soluble CR2 to immobilized C3d or iC3b are shown in Fig. 4, *C* and *D*, respectively. The kinetic constants for the interaction of CR2 with its ligands that we obtained from the global fitting analysis are summarized in Table I.

Binding of CR2 to a peptide corresponding to C3 amino acids K^{1187}-A^{1214}

In light of our observation that C3d interacts with CR2 in a complex manner and the controversy regarding the involvement of the C3 region comprising aa 1187–1214 in CR2 binding, we analyzed the binding of CR2 to a synthetic peptide carrying this amino acid

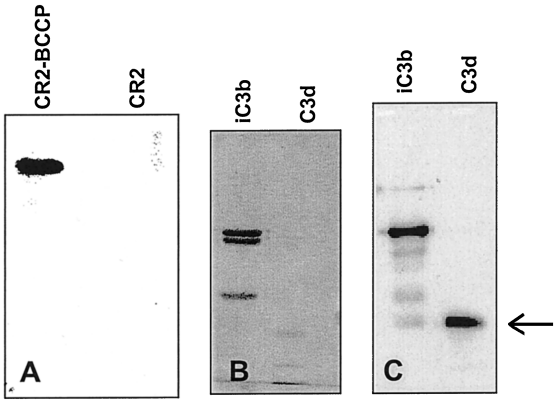

FIGURE 3. SDS-PAGE and Western blotting of the biotinylated CR2-BCCP and C3 fragments. *A*, Biotin was incorporated into CR2-BCCP in a reaction catalyzed by the enzyme BirA. *Lane 1*, Western blot of biotinylated CR2-BCCP, detected with peroxidase-labeled streptavidin. *Lane 2*, Nonbiotinylated CR2 control. *B* and *C*, PEO-maleimide biotin bound to Cys^{988} at the C3 thioester site. Biotinylated C3 was thereafter cleaved into iC3b and C3d (see *Materials and Methods*). *B*, Coomassie blue staining of biotinylated iC3b and C3d. Arrow indicates C3d position. *C*, Western blot of the biotinylated C3 fragments, probed with peroxidase-labeled streptavidin. The proteins were analyzed under reducing conditions.

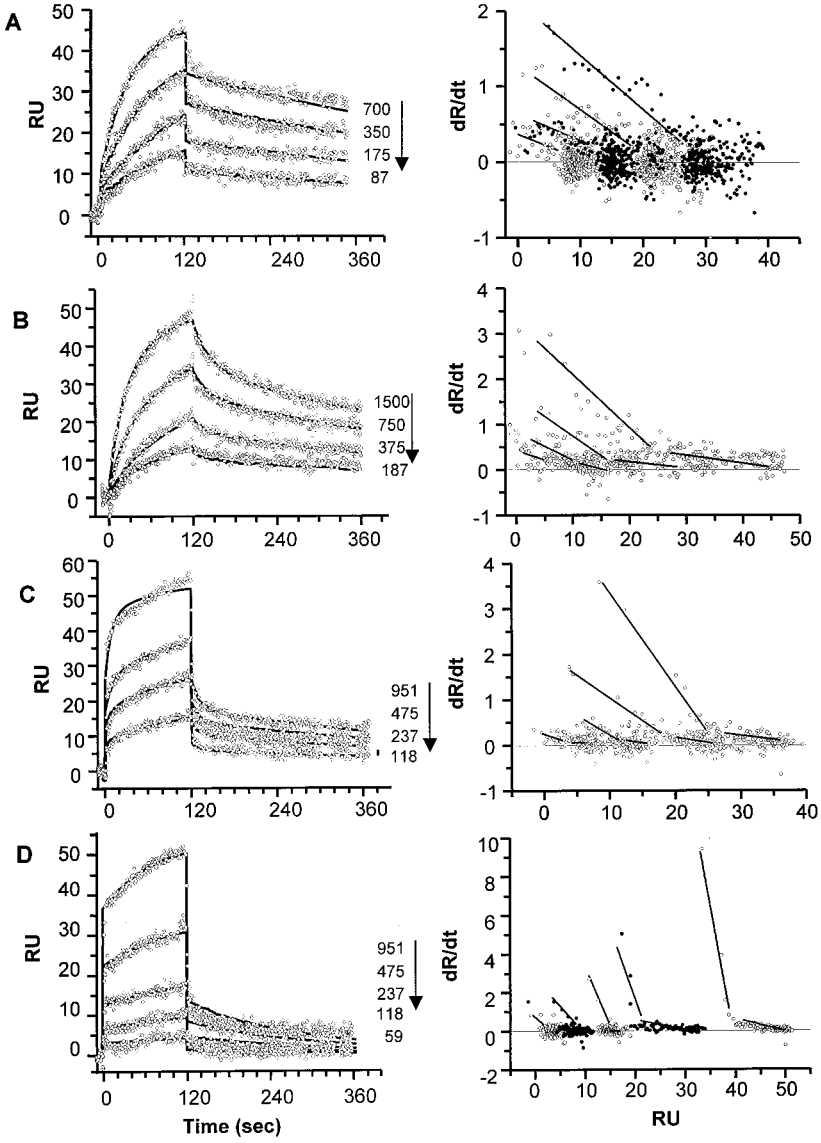

FIGURE 4. Analysis of the binding of CR2 to its ligands gp350, C3d, and iC3b by SPR. *Left*, Sensogram overlays for the interaction of immobilized CR2-BCCP with gp350 (470t) (*A*) and iC3b (*B*), as well as those for the interaction of soluble CR2 with immobilized C3d (*C*) and iC3b (*D*). The nanomolar concentration of injected analyte, is indicated at the right-hand side of the sensogram. Solid lines are the result of the global fitting analysis. gp350 (470t) binding to CR2 (*A*) fit a 1:1 Langmuir binding model, whereas binding of the C3 fragments to the receptor fit to a bivalent interaction. *Right*, Linear transformation of the association data. Solid lines were drawn to provide clarity and do not represent linear fits.

sequence (24). The $C3^{1187–1214}$ peptide (24) was biotinylated on its N terminus and immobilized on the Fc2 of a streptavidin sensor chip. As control we used an irrelevant biotinylated peptide, which was immobilized on Fc1. The experiment was performed in the presence of 75 mM NaCl in the running buffer to allow for better detection. Binding of CR2 to the $C3^{1187–1214}$ peptide was dose-dependent (Fig. 5). Furthermore, the interaction was inhibited by soluble C3d, but not by a control protein (BSA) (data not shown). Although global fitting of the data was not possible, these data indicate that the C3 region, 1187–1214, binds to CR2.

Effect of NaCl on the kinetics of CR2-ligand interaction

Recent availability of the x-ray structure of human C3d (30) and mutation analysis of charged residues of C3d (31) have highlighted the importance of ionic interactions in C3d-CR2 interactions. To understand the influence of ionic contacts on the kinetics of CR2-ligand interactions, we have studied these interactions at various salt concentrations using SPR technology.

In the present study we measured the binding of CR2 to its ligands at physiologic (150 mM) and half-physiologic (75 mM) ionic strength buffers. In all the interactions analyzed in this study, decreasing the amount of NaCl in the binding buffer lowered by ~4- or 5-fold the quantity of C3 fragments or gp350, respectively, that was required to obtain a similar response in PBS (data not shown). Therefore, a decrease in the salt concentration apparently facilitates the binding of CR2 to its ligands, by increasing the affinity of these interactions.

We then attempted to fit these binding data to a kinetic model. The binding of gp350 to immobilized CR2 and that of CR2 to immobilized C3d and iC3b fit well with a 1:1 and a bivalent interaction model, respectively (data not shown). Therefore, these data suggest that the mechanism of binding of CR2 to C3d, iC3b, and gp350 is not affected by the ionic strength of the buffer. The K_D values obtained from these analyses are presented in Table I.

To better understand the significance of these values for the binding of CR2 to C3d, we have overlaid the sensograms for the interaction of soluble CR2 with C3d in the presence of either 75 or 150 mM NaCl. As shown in Fig. 6, the total binding of 475 nM CR2 was increased by lowering the salt concentration. We then split the total binding curves into the components of a bivalent model. This strategy allowed us to analyze the parameter T_{50}, which is the time in the association phase at which the encounter and final complexes are equimolar, as defined by Lipschultz et al. (55). T_{50} at 75 mM NaCl was 40 s whereas at 150 mM NaCl T_{50}

Table I. *Kinetic values for the interaction of CR2 with its ligands gp350, iC3b, and C3d*[a]

Ligand	Analyte	k_{d1}(1/s)/ k_{a1}(1/M s)	SE (k_{d1}/k_{a1})	K_{D1}	k_{d2}(1/s)/ k_{a2}(1/M s)[b]	SE (k_{d2}/k_{a2})	$K_{D2}{}^{nM}$	χ^2	E. R_{max}[c]/ Calc. R_{max}[d](RU)
CR2	gp350	$1.5 \times 10^{-3}/3.3 \times 10^{4}$	$1.7 \times 10^{-5}/160$	45 nM	N.A.[e]	N.A.	N.A.	1.8	88/40
CR2	iC3b[f]	$0.0293/4.7 \times 10^{3}$	$8.2 \times 10^{-4}/32$	6.19 μM	$1.28 \times 10^{-3}/4148$	$2.52 \times 10^{-5}/61$	308	1.51	163/114
iC3b	CR2	$0.247/3.9 \times 10^{4}$	$4 \times 10^{-3}/8 \times 10^{2}$	6.3 μM	$1.52 \times 10^{-3}/2134$	$3.8 \times 10^{-5}/3.8$	712	1.7	238/193
C3d	CR2	$0.082/1.9 \times 10^{4}$	$6 \times 10^{-3}/1 \times 10^{3}$	4.3 μM	$1.1 \times 10^{-3}/4245.6$	$1.6 \times 10^{-9}/8.5$	259	2.37	828/127
CR2	gp350[f]	$5.5 \times 10^{-4}/1.2 \times 10^{5}$	$5.5 \times 10^{-6}/534$	4.6 nM	N.A.	N.A.	N.A.	1.35	88/40
C3d	CR2[f]	$0.202/7.24 \times 10^{4}$	$3.1 \times 10^{-3}/998$	2.8 μM	$8.28 \times 10^{-4}/3584$	$8.9 \times 10^{-6}/50$	231	1.67	828/112
iC3b	CR2[f]	$0.332/2.74 \times 10^{5}$	$6 \times 10^{-3}/5 \times 10^{3}$	1.2 μM	$5.9 \times 10^{-4}/1055$	$1.5 \times 10^{-5}/10$	559	2.39	238/139

[a] Data represent the average of duplicate experiments.
[b] k_{a2} (1/Ms) = k_{a2} (1/RUs) × 100 × (molecular weight of ligand).
[c] E. (expected) R_{max} = RU immobilized × molecular weight of analyte/molecular weight ligand.
[d] Calc. (calculated) R_{max} = R_{max} obtained in the global fitting analysis.
[e] N.A., Nonapplicable.
[f] Experiments performed at 75 mM NaCl.

was greater than the contact time. Thus, it appears that the initial charge-dependent binding is critical in the formation of stable CR2-C3d or CR2-iC3b complexes.

Binding of CR2 to C3c

The existence of kinetic differences between the binding of C3d and iC3b to CR2 led us to test the hypothesis that additional binding sites for CR2 may exist on C3c. C3c was immobilized on a sensor chip by amine-coupling chemistry, and soluble CR2 was allowed to interact with it. The experiment was performed under half ionic strength (75 mM NaCl) buffer conditions to allow better detection. Binding of CR2 to C3c was dose-dependent (Fig. 7*A*) and was inhibited by the presence of low molar excess of soluble C3c but not C3d (data not shown). The presence of traces of C3d on the C3c sample was examined with the reactivity of an anti-C3d monoclonal Ab (C3-19) in a Western blot assay (data not shown). The detection limit of this assay was 0.8 pmol of C3d, which represents <3% of the amount of C3c loaded on the gel. Thus, the C3c sample contained <3% of C3d. To further eliminate any possibility of presence of C3d, the binding response of two anti-C3d mAbs (mAb 130, mAb C3-19) to the sensor chip containing immobilized C3c was similar to that of a control Ab (mAb 72A1), and significantly lower that that of two anti-C3c Abs (C3-9, 133-H11) (Fig. 7*B*). All these data argue strongly against the possibility that the observed CR2 binding was due to the presence of traces of C3d in the C3c sample.

Effect of assay orientation on the iC3b-CR2 binding kinetics

To assess whether protein orientation had any effect on the kinetics of CR2-iC3b complex formation, we compared the binding of soluble CR2 to iC3b and vice versa, in the presence of 75 mM NaCl (Fig. 8). The initial association and dissociation phases occurred more rapidly when soluble CR2 bound to iC3b immobilized on the chip (Fig. 8*A*) than in the converse situation (Fig. 8*B*). This observation suggests that, indeed, experimental design may affect the interaction between CR2 and its ligands as a function of time.

Discussion

In the present study, we have used SPR technology to analyze the interaction of CR2 with its ligands, EBV gp350/220, C3d, and iC3b. Although the importance of these interactions is well established, the detailed nature of the molecular mechanisms involved is still unclear. Here, we have demonstrated that binding mechanism of CR2 varies with its ligands: its binding to gp350 follows a simple 1:1 model, whereas its binding to C3d and iC3b is more complex and suggests involvement of more than one site in these interactions. Furthermore, our data show kinetic differences between the binding of iC3b and C3d to CR2, which suggest that the regions of iC3b and C3d that are involved in the interaction with CR2 may not be the same or may be differently exposed in the two molecules.

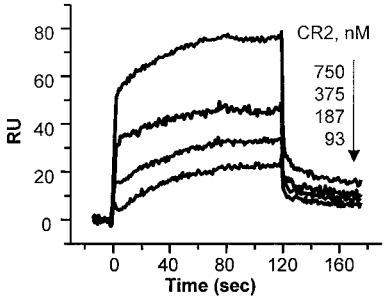

FIGURE 5. Binding of CR2 to $C3^{1187–1214}$ peptide. Overlay plot showing binding of soluble CR2 to immobilized $C3^{1187–1214}$ peptide. Several concentrations of CR2 were injected over a streptavidin sensor chip containing a biotinylated control peptide immobilized on Fc1, and biotinylated $C3^{1187–1214}$ peptide on Fc2. Data were collected with 75 mM NaCl present in the binding buffer. The concentration (nanomoles) of injected CR2, is indicated at right.

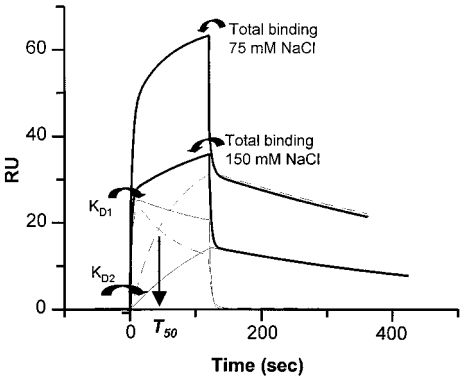

FIGURE 6. Effect of NaCl concentration on the binding of CR2 to immobilized C3d as analyzed by SPR. Overlay plot of the binding of 475 nM CR2 to immobilized C3d in the presence of 75 or 150 mM NaCl in the binding buffer. BIAevaluation software was used to view the two binding components, K_{D1} and $K_{D2,}$ of these interactions. Thick lines represent the total binding. The thin solid lines represent the K_{D1} and K_{D2} at 150 mM NaCl; the thin dashed lines represent K_{D1} and K_{D2} at 75 mM NaCl.

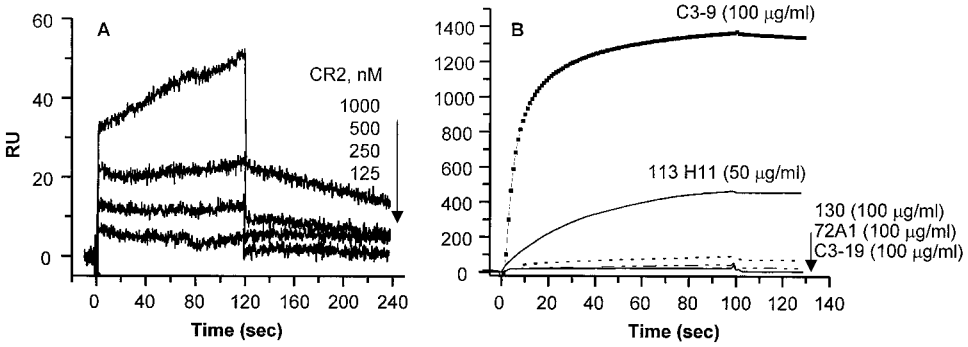

FIGURE 7. Binding of CR2 to C3c. C3c was immobilized on the Fc2 of a CM5 chip by amine-coupling chemistry, whereas Fc1 was used as a blank control. *A*, Overlay plot showing binding of soluble CR2 to immobilized C3c protein. Several concentrations of CR2 were injected in the presence of 75 mM NaCl in the binding buffer. The concentration (nanomoles) of injected CR2, is indicated at right. *B*, Overlay plot of the binding of mAbs anti-C3d (130 and C3-19); anti-C3c (C3-9 and 113 H11), and anti-gp350 (72A1) to immobilized C3c protein. Several concentrations of each of the Abs were injected, but only the highest is shown for better clarity.

In an attempt to mimic the actual in vivo orientation of these proteins, we have biotinylated them at key residues, i.e, the Cys^{988} residue that participates in the thioester bond formation in C3 (45, 56), and the C-terminal end of CR2. The immobilization of biotinylated C3d/iC3b on a streptavidin surface (i.e., the BIAcore chip) was intended to simulate the deposition of C3 onto activating particles. Likewise, immobilization of a CR2 molecule containing biotin at its C terminus mimicked anchoring on the cell surface. Orientation of proteins in this way provided an advantage over the random amine-coupling method generally used in SPR-based assays, because it produced a homogeneous ligand surface that facilitated the measurement of homogeneous binding constants.

To study the interaction of CR2 with EBV gp350, we expressed a truncated form of gp350/220, consisting of residues 1–470. This truncated molecule had previously been shown to inhibit EBV binding to CR2 (23). The SPR data obtained for this CR2-gp350 (470t) interaction showed a close fit to 1:1 Langmuir binding model (Fig. 4). The apparent K_D value obtained for this interaction was 45 nM (Table I). Affinities for the interaction of gp350/220 with CR2 have been previously determined by equilibrium binding in two different experimental settings. Tanner and coworkers (23) examined the ability of gp350/220 to inhibit the binding of ^{125}I-labeled gp350/220 to CR2-expressing cells (Raji), and Moore and coworkers (57) studied the binding of soluble CR2 to gp350/220 by measuring the changes in mobility of the CR2-gp350/220 complexes in the ultracentrifuge as a function of ligand concentration. The K_D values obtained by the two groups were 12 and 3.2 nM, respectively. The differences observed between these studies could reflect different affinities of CR2 for gp350/220 when present on the cell surface or in solution. In our case, the differences in K_D values observed between the present study (CR2 anchored to the sensor chip; K_D = 45 nM) and the previous study (23) (CR2 present on cell surface; K_D = 12 nM) could be due to truncation of the protein used in our study. We used a protein truncated at residue 470, whereas the previous studies used the entire molecule. Therefore, these data suggest that other regions in gp350 may be directly involved or influencing its binding to CR2.

Our analysis of the binding between CR2 and its natural ligands C3d and iC3b revealed that these interactions do not follow a simple 1:1 binding model (Fig. 4). We eliminated surface heterogeneity by implementing the directed orientation of the immobilized ligands. Additionally, the fact that the gp350 binding data fit a 1:1 model both argue strongly against the influence of experimental artifacts in these data. Linear transformation of the association and dissociation data showed nonlinear plots (Fig. 4). These nonlinear binding curves could reflect multiple binding sites with different affinities, cooperativity, or more complex models. Global fitting analysis of the binding data suggested that the interaction between CR2 and C3d/iC3b follows a bivalent model (Fig. 4). It is possible that two regions of the C3d/iC3b molecule actually interact with two regions of the CR2 molecule; in this case the stoichiometry of the complex would be 1:1, which is in accordance with the previous findings of Moore and coworkers (57).

Several lines of evidence support a multiple site interaction model for C3d/iC3b binding to CR2. First, it has been shown that two different regions within SCR 1 and 2 of CR2 are involved in its interaction with C3 (22, 53). Furthermore, data from our laboratory and others have indicated that at least two regions of human C3d are involved in its interaction with CR2 (24, 29, 31, 54). However, involvement of the region in C3 comprising aa 1199–1210 in binding to CR2 has been disputed (29, 31). To reassess this interaction using SPR technology, we performed a direct binding assay. We observed that CR2 binds to a synthetic peptide with the C3 sequence ^{1187}K F L T T A K D L N R W E D P G K Q L Y

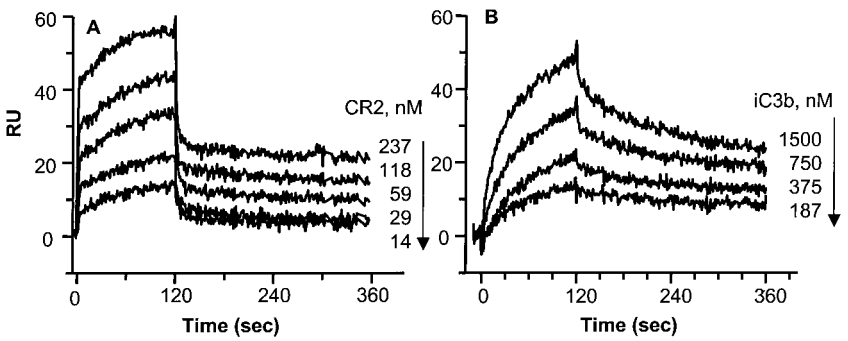

FIGURE 8. Binding of CR2 to immobilized iC3b and vice versa, as analyzed by SPR overlay plots of the binding of soluble CR2 to immobilized iC3b (*A*) and immobilized CR2 to soluble iC3b (*B*). Data were collected with 75 mM NaCl present in the binding buffer.

N V E A T S Y A^{1214} (24) (Fig. 5). The binding data could not be fit to any kinetic model, but it allowed us to observe that the dissociation of CR2 from C3$^{1187–1214}$ appeared to occur much faster than that from C3d (in the same buffer conditions). This suggests that other regions in C3d may be involved in its interaction with the receptor, possibly stabilizing the complex. In fact, when we attempted to competitively inhibit the binding of soluble CR2 to immobilized C3d with the C3$^{1187–1214}$ peptide, no inhibition of the CR2-C3d interaction could be observed (data not shown), suggesting that other regions on C3d also interact with the receptor. Alternatively, correct orientation of the peptide may be necessary for it to bind to CR2.

The data obtained in this study (Fig. 6) and in previous studies (31, 57) clearly indicate that the binding of C3d to CR2 is highly dependent on ionic interactions. SPR data obtained in the present study indicate the involvement of two components in the C3d-CR2 interaction (Fig. 4, *right panel*). To elucidate the influence of ionic interactions on these components we obtained T_{50} values (the time required to achieve an equimolar distribution of initial and final complexes) for binding of C3d to CR2 at physiologic and half-physiologic ionic strengths. We observed that lowering the amount of salt reduced the time required for the onset of secondary contacts in the interaction (Fig. 6). This finding suggests that some or all of the charged cluster of amino acids on C3d (E37, E39, E160, D163, and E166) that are known to influence CR2 binding when absent (31) may participate in the second component of the interaction. In the absence of these residues, binding of CR2 to C3d may have such fast association and dissociation rates that it may not be detected in assays that do not involve chemical cross-linking or SPR. In fact, our SPR data revealed that dissociation of CR2 from the C3$^{1187–1214}$ peptide occurs much faster than its dissociation from C3d (Figs. 5 and 6). Alternatively, the charged cluster of residues in C3d may cooperatively contribute to the interaction.

A careful analysis of our SPR data indicates that the interactions of C3d and iC3b with CR2 are not identical. Although both interactions seemed to follow a complex model, there appear to be significant differences between the binding of soluble CR2 to immobilized C3d and iC3b. For example, the on-rates of both the first and second components of C3d and iC3b differed from each other by >2-fold (Table I). Our results indicate that the interactions of C3d and iC3b with CR2, although similar, appear to involve some notable differences. This may be due to the participation of the CR2-interacting iC3b residues located outside the C3d region (25). We observed that CR2 interacted with C3c when the latter was immobilized in a sensor chip (Fig. 7). This result points toward the presence of CR2-interacting residues on the C3c fragment that may explain the differences observed between C3d and iC3b binding to CR2. Interestingly, this interaction could be inhibited by soluble C3c (data not shown), which suggests that the CR2 binding residues in C3c are exposed when in soluble C3c, i.e., immobilization of C3c did not significantly alter the conformation of these residues. High amounts (2800 RU) of C3c were immobilized in the chip in a random orientation, two factors that may induce surface heterogeneity. Therefore, we did not attempt to fit the CR2-C3c binding data to any kinetic model.

In addition to the presence of contact sites on C3c, other factors may contribute to differential binding of iC3b and C3d to CR2. Several residues in the C3d region of iC3b may be less accessible to CR2 as compared with those of C3d. Evidence suggesting that such steric hindrance may exist was presented in a study that used mAb 130 (58, 59). This Ab, which recognizes a neoantigenic determinant that is expressed when C3b is cleaved to iC3b and inhibits CR2 binding (24), was found to bind C3d better than iC3b (59).

Although it is clear from our data that C3d/iC3b-CR2 interactions do not follow simple 1:1 interactions and that the data show two components (Fig. 4, *right panel*) and fit well with a bivalent interaction model (Fig. 4, *left panel*), the complexity of the model precludes us from concluding that these are bivalent interactions, because increasing the complexity of a model increases the potential for multiple local minima in the χ^2 function that decrease the stability of the fitting procedure. However, we have shown in this study that multiple regions in C3 interact directly with the receptor.

It is also conceivable that CR2 has different affinities for soluble or surface-bound C3 fragments (i.e., those bound to the activating particle at their thioester site). In this study we have examined the effect of ligand orientation on the binding kinetics of the iC3b-CR2 interaction. We observed differences in the on- and off-rates of iC3b, depending on whether it was oriented on the surface or present in solution. Complex formation and dissociation was initially faster when iC3b was immobilized than when it was presented in soluble form. Immobilization of iC3b through Cys^{988}, which is involved in the thioester bond formation, may render the CR2-interacting residues more accessible. Similarly, differential expression of various epitopes on fluid-phase vs surface-bound C3 has already been proposed. Nilsson and coworkers have found that the reactivity of several mAbs recognizing the C3 α-chain differ when the C3 fragments are in fluid phase or surface-bound (60).

In summary, we have used SPR technology to gain insight into the interaction between CR2 and its ligands. We have found that in contrast to gp350 (470t), C3d and iC3b appear to bind to CR2 in a complex manner.

Acknowledgments

We thank Y. H. Shahan for excellent technical assistance; D. McClellan for editorial assistance; Dr. Michael Holers (Department of Medicine and Immunology, University of Colorado Health Science Center, Denver, CO) for providing the CR2-expressing clone; Dr. Dorothy Beckett (Department of Chemistry and Biochemistry, University of Maryland, College Park, MD) for providing the BirA-expressing clone. We also thank Dr. C. Whitbeck for help with protein expression in the baculovirus system, Dr. A. Rux for help on SPR experiments, and Drs. G. H. Cohen and R. J. Eisenberg for the use of their BIAcore X system in the initial experiments.

References

1. Tsoukas, C. D., and J. D. Lambris. 1993. Expression of EBV/C3d receptors on T cells: biological significance. *Immunol. Today 14:56.*
2. Krych, M., J. P. Atkinson, and V. M. Holers. 1992. Complement receptors. *Curr. Opin. Immunol. 4:8.*
3. Fearon, D. T., and J. M. Ahearn. 1990. Complement receptor type 1 (C3/C4b receptor; CD35) and complement receptor type 2 (C3d/Epstein-Barr virus receptor; CD21). *Curr. Top. Microbiol. Immunol. 153:83.*
4. Lambris, J. D. 1990. *The Third Component of Complement: Chemistry and Biology.* Springer-Verlag, Berlin.
5. Ahearn, J. A., and A. M. Rosengard, 1998:Complement receptors. In *The Human Complement System in Health and Disease.* J. E. Volanakis and M. Frank, eds. Marcel Dekker, New York.
6. Fujisaku, A., J. B. Harley, M. B. Frank, B. A. Gruner, B. Frazier, and V. M. Holers. 1989. Genomic organization and polymorphisms of the human C3d/Epstein-Barr virus receptor. *J. Biol. Chem. 264:2118.*
7. Hourcade, D., V. M. Holers, and J. P. Atkinson. 1989. The regulators of complement activation (RCA) gene cluster. *Adv. Immunol. 45:381.*
8. Carroll, M. C. 1998. The role of complement and complement receptors in induction and regulation of immunity. *Annu. Rev. Immunol. 16:545.*
9. Noorchashm, H., D. J. Moore, Y. K. Lieu, N. Noorchashm, A. Schlachterman, H. K. Song, J. D. Lambris, C. F. Barker, and A. Naji. 1999. Contribution of the innate immune system to autoimmune diabetes: a role for the CR1/CR2 complement receptors. *Cell. Immunol. 195:75.*
10. Tsokos, G. C., J. D. Lambris, F. D. Finkelman, E. D. Anastassiou, and C. H. June. 1990. Monovalent ligands of complement receptor 2 inhibit whereas polyvalent ligands enhance anti-Ig-induced human B cell intracytoplasmic free calcium concentration. *J. Immunol. 144:1640.*
11. Thyphronitis, G., T. Kinoshita, K. Inoue, J. E. Schweinle, G. C. Tsokos, E. S. Metcalf, F. D. Finkelman, and J. E. Balow. 1991. Modulation of mouse complement receptor-1 and receptor-2 suppresses antibody responses in vivo. *J. Immunol. 147:224.*
12. Carroll, M. C., and A. P. Prodeus. 1998. Linkages of innate and adaptive immunity. *Curr. Opin. Immunol. 10:36.*

13. Dempsey, P. W., M. E. D. Allison, S. Akkaraju, C. C. Goodnow, and D. T. Fearon. 1996. C3d of complement as a molecular adjuvant: bridging innate and acquired immunity. *Science 271:348.*
14. Ross, T. M., Y. Xu, R. A. Bright, and H. L. Robinson. 2000. C3d enhancement of antibodies to hemagglutinin accelerates protection against influenza virus challenge. *Nat. Immunol. 2:121.*
15. Nemerow, G. R., C. Mold, V. K. Schwend, V. Tollefson, and N. R. Cooper. 1987. Identification of gp350 as the viral glycoprotein mediating attachment of Epstein-Barr virus (EBV) to the EBV/C3d receptor of B cells: sequence homology of gp350 and C3 complement fragment C3d. *J. Virol. 61:1416.*
16. Tanner, J., J. Weis, D. Fearon, Y. Whang, and E. Kieff. 1987. Epstein-Barr virus gp350/220 binding to the B lymphocyte C3d receptor mediates adsorption, capping, and endocytosis. *Cell 50:203.*
17. Frade, R., M. Barel, B. Ehlin-Henriksson, and G. Klein. 1985. gp140, the C3d receptor of human B lymphocytes, is also the Epstein-Barr virus receptor. *Proc. Natl. Acad. Sci. USA 82:1490.*
18. Servis, C., and J. D. Lambris. 1989. C3 synthetic peptides support growth of human CR2-positive lymphoblastoid B cells. *J. Immunol. 142:2207.*
19. Bohnsack, J. F., and N. R. Cooper. 1988. CR2 ligands modulate human B cell activation. *J. Immunol. 141:2569.*
20. Goeckeritz, B. E., A. Lees, Q. Vos, G. C. Tsokos, K. Kuhlbusch, and J. J. Mond. 2000. Enhanced and sustained activation of human B cells by anti-immunoglobulin conjugated to the EBV glycoprotein gp350. *Eur. J. Immunol. 30:969.*
21. Lowell, C. A., L. B. Klickstein, R. H. Carter, J. A. Mitchell, D. T. Fearon, and J. M. Ahearn. 1989. Mapping of the Epstein-Barr virus and C3dg binding sites to a common domain on complement receptor type 2. *J. Exp. Med. 170:1931.*
22. Molina, H., C. Brenner, S. Jacobi, J. Gorka, J. C. Carel, T. Kinoshita, and V. M. Holers. 1991. Analysis of Epstein-Barr virus-binding sites on complement receptor 2 (CR2/CD21) using human-mouse chimeras and peptides: at least two distinct sites are necessary for ligand-receptor interaction. *J. Biol. Chem. 266: 12173.*
23. Tanner, J., Y. Whang, J. Sample, A. Sears, and E. Kieff. 1988. Soluble gp350/220 and deletion mutant glycoprotein block Epstein-Barr virus adsorption to lymphocytes. *J. Virol. 62:4452.*
24. Lambris, J. D., V. S. Ganu, S. Hirani, and H. J. Müller-Eberhard. 1985. Mapping of the C3d receptor (CR2)-binding site and a neoantigenic site in the C3d domain of the third component of complement. *Proc. Natl. Acad. Sci. USA 82:4235.*
25. Esparza, I., J. D. Becherer, J. Alsenz, A. De la Hera, Z. Lao, C. D. Tsoukas, and J. D. Lambris. 1991. Evidence for multiple sites of interaction in C3 for complement receptor type 2 (C3d/EBV receptor, CD21). *Eur. J. Immunol. 21:2829.*
26. Frade, R., J. Hermann, and M. Barel. 1992. A 16 amino acid synthetic peptide derived from human C3d triggers proliferation and specific tyrosine phosphorylation of transformed CR2-positive human lymphocytes and of normal resting lymphocytes-B. *Biochem. Biophys. Res. Commun. 188:833.*
27. Lou, D., and H. Kohler. 1998. Enhanced molecular mimicry of CEA using photoaffinity crosslinked C3d peptide. *Nat. Biotechnol. 16:458.*
28. Kalli, K. R., J. M. Ahearn, and D. T. Fearon. 1991. Interaction of iC3b with recombinant isotypic and chimeric forms of CR2. *J. Immunol. 147:590.*
29. Diefenbach, R. J., and D. E. Isenman. 1995. Mutation of residues in the C3dg region of human complement component C3 corresponding to a proposed binding site for complement receptor type 2 (CR2, CD21) does not abolish binding of iC3b or C3dg to CR2. *J. Immunol. 154:2303.*
30. Nagar, B., R. G. Jones, R. J. Diefenbach, D. E. Isenman, and J. M. Rini. 1998. X-ray crystal structure of C3d: a C3 fragment and ligand for complement receptor 2. *Science 280:1277.*
31. Clemenza, L., and D. E. Isenman. 2000. Structure-guided identification of C3d residues essential for its binding to complement receptor 2 (CD21). *J. Immunol. 165:3839.*
32. Holers, V. M., G. F. Hollis, B. D. Schwartz, R. J. Evans, J. Strauss-Schoenberger, J. C. Carel, D. L. Barney, B. Li, J. Stafford-Hollis, and P. E. Lacy. 1993. Induction of peri-insulitis but not diabetes in islet transplants expressing a single foreign antigen: a multi-stage model of disease. *J. Immunol. 151:5041.*
33. Hedrick, J. A., D. Watry, C. Speiser, P. O'Donnelli, J. D. Lambris, and C. D. Tsoukas. 1992. Interaction between Epstein-Barr virus and a T cell line (HSB-2) via a receptor phenotypically distinct from complement receptor type 2. *Eur. J. Immunol. 22:1123.*
34. Tessier, D. C., D. Y. Thomas, H. E. Khouri, F. Lalibertie, and T. Vernet. 1991. Enhanced secretion from insect cells of a foreign protein fused to the honeybee melittin signal peptide. *Gene 98:177.*
35. Blattner, F. R., G. Plunkett III, C. A. Bloch, N. T. Perna, V. Burland, M. Riley, J. Collado-Vides, J. D. Glasner, C. K. Rode, G. F. Mayhew, et al. 1997. The complete genome sequence of *Escherichia coli* K-12. *Science 277:1453.*
36. Xu, Y., and D. Beckett. 1997. Biotinyl-5′-adenylate synthesis catalyzed by *Escherichia coli* repressor of biotin biosynthesis. *Methods Enzymol. 279:405.*
37. Lambris, J. D., N. J. Dobson, and G. D. Ross. 1980. Release of endogenous C3b inactivator from lymphocytes in response to triggering membrane receptors for β1H globulin. *J. Exp. Med. 152:1625.*
38. Hsiung, L., A. N. Barclay, M. R. Brandon, E. Sim, and R. R. Porter. 1982. Purification of human C3b inactivator by monoclonal-antibody affinity chromatography. *Biochem. J. 203:293.*
39. Alsenz, J., T. F. Schulz, J. D. Lambris, R. B. Sim, and M. P. Dierich. 1985. Structural and functional analysis of the complement component factor H with the use of different enzymes and monoclonal antibodies to factor H. *Biochem. J. 232:841.*
40. Nilsson, U. R., R. J. Mandle, and J. A. McConnell-Mapes. 1975. Human C3 and C5: subunit structure and modification by trypsin and C42–C423. *J. Immunol. 114:815.*
41. Becherer, J. D., and J. D. Lambris. 1988. Identification of the C3b receptor-binding domain in third component of complement. *J. Biol. Chem. 263:14586.*
42. Sahu, A., S. N. Isaacs, A. M. Soulika, and J. D. Lambris. 1998. Interaction of vaccinia virus complement control protein with human complement proteins: factor I-mediated degradation of C3b to iC3b(1) inactivates the alternative complement pathway. *J. Immunol. 160:5596.*
43. Fan, X., and R. C. Beavis. 1993. Growing protein-doped sinaptic acid crystals for laser-desorption: an alternative preparation method for difficult samples 231. *Org. Mass Spectrom. 28:1424.*
44. Sahu, A., T. R. Kozel, and M. K. Pangburn. 1994. Specificity of the thioester-containing reactive site of human C3 and its significance to complement activation. *Biochem. J. 302:429.*
45. Law, S. K. A., and A. W. Dodds. 1997. The internal thioester and the covalent binding properties of the complement proteins C3 and C4. *Protein Sci. 6:263.*
46. Sahu, A., A. M. Soulika, D. Morikis, L. Spruce, W. T. Moore, and J. D. Lambris. 2000. Binding kinetics, structure-activity relationship, and biotransformation of the complement inhibitor compstatin. *J. Immunol. 165:2491.*
47. Casasnovas, J. M., and T. A. Springer. 1995. Kinetics and thermodynamics of virus binding to receptor: studies with rhinovirus, intercellular adhesion molecule-1 (ICAM-1), and surface plasmon resonance. *J. Biol. Chem. 270:13216.*
48. Morton, T. A., D. B. Bennett, E. R. Appelbaum, D. M. Cusimano, K. O. Johanson, R. E. Matico, P. R. Young, M. Doyle, and I. M. Chaiken. 1994. Analysis of the interaction between human interleukin-5 and the soluble domain of its receptor using a surface plasmon resonance biosensor. *J. Mol. Recognit. 7:47.*
49. Hessing, M., H. B. Vanschijndel, W. M. J. Vangrunsven, H. Wolf, and J. M. Middeldorp. 1992. Purification and quantification of recombinant Epstein-Barr viral glycoproteins gp350/220 from Chinese hamster ovary cells. *J. Chromatogr. 599:267.*
50. Nuebling, C. M., M. Buck, H. Boos, A. Vondeimling, and N. Muellerlantzsch. 1992. Expression of Epstein-Barr virus membrane antigen-gp350/220 in *E. coli* and in insect cells. *Virology 191:443.*
51. Beckett, D., E. Kovaleva, and P. J. Schatz. 1999. A minimal peptide substrate in biotin holoenzyme synthetase-catalyzed biotinylation. *Protein Sci. 8:921.*
52. Molina, H., C. Brenner, S. Jacobi, J. Gorka, J. C. Carel, T. Kinoshita, and V. M. Holers. 1991. Analysis of Epstein-Barr virus-binding sites on complement receptor 2 (CR2/CD21) using human-mouse chimeras and peptides: at least two distinct sites are necessary for ligand-receptor interaction. *J. Biol. Chem. 266: 12173.*
53. Molina, H., S. J. Perkins, J. Guthridge, J. Gorka, T. Kinoshita, and V. M. Holers. 1995. Characterization of a complement receptor 2 (CR2, CD21) ligand binding site for C3: an initial model of ligand interaction with two linked short consensus repeat modules. *J. Immunol. 154:5426.*
54. Irani, V. R., and J. D. Lambris. 1999. Studies on the interaction of C3dg with CR2. *FASEB J. 13:A282.*
55. Lipschultz, C. A., Y. Li, and S. Smith-Gill. 2000. Experimental design for analysis of complex kinetics using surface plasmon resonance. *Methods 20:310.*
56. Pangburn, M. K. 1992. Spontaneous thioester bond formation in α2-macroglobulin, C3 and C4. *FEBS Lett. 308:280.*
57. Moore, M. D., R. G. DiScipio, N. R. Cooper, and G. R. Nemerow. 1989. Hydrodynamic, electron microscopic and ligand binding analysis of the Epstein-virus/C3dg receptor (CR2). *J. Biol. Chem. 264:20576.*
58. Tamerius, J. D., M. K. Pangburn, and H. J. Müller-Eberhard. 1982. Selective inhibition of functional sites of cell-bound C3b by hybridoma-derived antibodies. *J. Immunol. 128:512.*
59. Aguado, M. T., J. D. Lambris, G. C. Tsokos, R. Burger, D. Bitter-Suermann, J. D. Tamerius, F. J. Dixon, and A. N. Theofilopoulos. 1985. Monoclonal antibodies against complement 3 neoantigens for detection of immune complexes and complement activation: relationship between immune complex levels, state of C3, and numbers of receptors for C3b. *J. Clin. Invest. 76:1418.*
60. Nilsson, B., D. Grossberger, E. K. Nilsson, P. Riegert, D. J. Becherer, U. R. Nilsson, and J. D. Lambris. 1992. Conformational differences between surface-bound and fluid-phase complement-component-C3 fragments: epitope mapping by cDNA expression. *Biochem. J. 282:715.*